Hydrothermal Synthesis of Organic−Inorganic Hybrid Materials: Network Structures of the Bimetallic Oxides [M(Hdpa)$_2$V$_4$O$_{12}$] (M = Co, Ni, dpa = 4,4′-Dipyridylamine)

Robert L. LaDuca, Jr.,*,† Randy S. Rarig, Jr.,‡ and Jon Zubieta*,‡

Department of Chemistry, Syracuse University, Syracuse, New York 13244,
and Department of Chemistry and Physics, King's College, Wilkes-Barre, Pennsylvania 18711

Received February 29, 2000

The hydrothermal reactions of $MCl_2 \cdot 6H_2O$ (M = Co, Ni) $NaVO_3$, 4,4′-dipyridylamine (dpa), and H_2O yield materials of the type [M(Hdpa)$_2$V$_4$O$_{12}$] (M = Co (**1**), Ni (**2**)). The two-dimensional structures of **1** and **2** are constructed from bimetallic oxide networks $\{MV_4O_{12}\}_n^{2n-}$ with monodentate Hdpa$^+$ projecting the protonated ring into the interlamellar region. The oxide network may be described as ruffled chains of corner-sharing $\{VO_4\}$ tetrahedra linked by $\{NiO_4N_2\}$ octahedra into the two-dimensional assembly. Crystal data: $C_{10}H_{10}Co_{0.5}N_3O_6V_2$ (**1**), monoclinic $P2_1/c$, $a = 10.388(1)$ Å, $b = 7.6749(7)$ Å, $c = 16.702(2)$ Å, $\beta = 102.516(1)°$, $Z = 4$. $C_{10}H_{10}N_3Ni_{0.5}O_6V_2$ (**2**), monoclinic, $P2_1/c$, $c = 10.3815(2)$ Å, $b = 7.7044(2)$ Å, $c = 16.6638(4)$ Å, $\beta = 102.573(1)°$, $Z = 4$.

The remarkable compositional range and structural variety of inorganic oxides endows these materials with a gamut of useful physical properties, giving rise to applications in areas spanning heavy construction to microelectronics.[1,2] Despite such widespread utility, the synthetic design of the structure of oxide materials remains a challenge in solid-state chemistry.[3,4] Binary metal oxides, for example, typically exhibit one or a small number of thermodynamically stable modifications, providing a limited scope for synthetic design. However, if the paradigm is shifted from thermodynamic to kinetic control, it is possible to prepare metastable structures and to direct the synthetic process. Furthermore, at the more benign temperatures and conditions adopted for the preparation of such metastable oxides, organic molecules may be introduced as structure-directing components. In fact, it is now well-documented that organic molecules can profoundly alter oxide microstructures, thus offering a powerful tool for the design of new materials.[5]

The classical examples of templating of inorganic oxides by small organic molecules are represented by zeolites, where the organic component is entrained within the crystallizing inorganic framework during hydrothermal synthesis.[6,7] This useful strategy for the modification of inorganic oxide substructures has been extended to the design of families of materials, such as mesoporous oxides of the MCM-41 family[8,9] and oxometal phosphates,[10,11] as well as underlying nature's remarkable mineral-based materials.[12,13]

Expanding on this approach, we have begun to develop the structural chemistry of molybdenum and vanadium oxides[14−23] in combination with secondary metal−ligand complex cations, which serve to provide charge compensation for the negatively charged oxide substructure of the resultant composite material, as well as fulfilling space-filling and structure-directing roles. These hybrid materials manifest the structural influences both of the coordination preferences of the secondary metal site and of the geometric constraints of the ligand. Thus, the secondary metal−ligand moiety may adopt a variety of substructural motifs: (a) isolated coordination complex cation, as in the two-dimensional vanadate phase [Cu(en)$_2$][V$_6$O$_{14}$];[14] (b) a polymeric

† King's College.
‡ Syracuse University.

(1) Cheetham, A. J. *Science* **1996**, *264*, 794 and references therein.
(2) Bruce, D. W.; O'Hare, D., Eds. *Inorganic Materials*; Wiley: Chichester, 1992.
(3) Mallouk, T. E.; Lee, H. *J. Chem. Educ.* **1990**, *67*, 829.
(4) Behrens, P. *Angew. Chem., Int. Ed. Engl.* **1996**, *35*, 515.
(5) (a) Stupp, S. I.; Braun, P. V. *Science* **1997**, *277*, 1242 and references therein. (b) Chesnut, D. J.; Hagrman, D.; Zapf, P. J.; Hammond, R. P.; LaDuca, R. L., Jr.; Haushalter, R. C.; Zubieta, J. *Coord. Chem. Rev.* **1999**, *190−192*, 757.
(6) Occelli, M. L.; Robson, H. C. *Zeolite Synthesis*; American Chemical Society: Washington, DC, 1989.
(7) Davis, M. E.; Katz, A.; Ahmad, W. R. *Chem. Mater*. **1996**, *8*, 1820.
(8) Kresge, C. T.; Leonowicz, M. E.; Roth, W. J.; Vartuli, J. C.; Beck, J. S. *Nature (London)* **1997**, *359*, 710.
(9) Behrens, P.; Stucky, G. *Angew. Chem., Int. Ed. Engl.* **1993**, *32*, 696.
(10) Khan, M. I.; Meyer, L. M.; Haushalter, R. C.; Schweitzer, C. L.; Zubieta, J.; Dye, J. L. *Chem. Mater*. **1996**, *8*, 43 and references therein.
(11) Cheetham, A. K.; Férey, G.; Loiseau, T. *Angew. Chem., Int. Ed. Engl.* **1999**, *38*, 3268.
(12) Mann, S.; Burkett, S. L.; Davis, S. A.; Fowler, C. E.; Mendelson, N. H.; Seins, S. D.; Walsh, D.; Whilton, N. T. *Chem. Mater.* **1997**, *9*, 2300 and references therein.
(13) Oliver, S.; Coombs, N.; Ozin, G. A. *Adv. Mater*. **1995**, *7*, 931.
(14) Zhang, Y.; DeBord, J. R. D.; O'Connor, C. J.; Haushalter, R. C.; Clearfield, A.; Zubieta, J. *Angew. Chem., Int. Ed. Engl*. **1996**, *35*, 989.
(15) Hagrman, P. J.; Bridges, C.; Greedan, J. E.; Zubieta, J. *J. Chem. Soc., Dalton Trans.* **1999**, 2901.
(16) LaDuca, R. L., Jr.; Finn, R.; Zubieta, J. *Chem. Commun.* **1999**, 1669.
(17) Hagrman, P. J.; Hagrman, D.; Zubieta, J. *Angew. Chem., Int. Ed. Engl.* **1999**, *38*, 2638 and references therein.
(18) Hagrman, D.; Zubieta, C.; Rose, D. J.; Zubieta, J.; Haushalter, R. C. *Angew. Chem., Int. Ed. Engl.* **1997**, *36*, 873.
(19) Hagrman, D.; Sangregorio, C.; O'Connor, C. J.; Zubieta, J. *J. Chem. Soc., Dalton Trans*. **1998**, 3707.
(20) Hagrman, D.; Hammond, R. P.; Haushalter, R.; Zubieta, J. *Chem. Mater*. **1998**, *10*, 2091.
(21) Hagrman, D.; Warren, C. J.; Haushalter, R. C.; Seip, C.; O'Connor, C. J.; Rarig, R. S., Jr.; Johnson, K. M., III; LaDuca, R. L., Jr.; Zubieta, J. *Chem. Mater*. **1998**, *10*, 3294.
(22) Hagrman, D.; Zubieta, J. *Compt. Rend.*, in press.
(23) Hagrman, D.; Hagrman, P.; Zubieta, J. *Inorg. Chim. Acta*, in press.

10.1021/ic000224i CCC: $20.00
Published on Web 01/13/2001

coordination complex cation with a one-, two-, or three-dimensional substructure, of which [{Cu(4,4′-bpy)}$_4$Mo$_8$O$_{26}$],[18] [Ni(dpa)$_2$MoO$_4$] (dpa = dipyridylamine),[24] and [{Fe(tpypor)}$_3$Fe(Mo$_6$O$_{19}$)$_2$],[25] respectively, are representative examples; and (c) integral components of bimetallic oxide chain, network, or framework substructures, as in [{Fe(2,2′-bpy)}$_2$Mo$_3$O$_{12}$],[26] [Co(2,2′-bpy)Mo$_3$O$_{10}$],[27] and [Cu(pyz)$_{0.5}$MoO$_4$],[21] respectively.

As an extension of this synthetic approach to organic−inorganic hybrid oxides, we have begun to investigate the chemistry of the M(II)−vanadate−4,4′-dipyridylamine (dpa) family of oxides. The dpa ligand is particularly attractive in this context, in part by virtue of the nonlinear orientation of the nitrogen donor groups in contrast to the more extensively studied 4,4′-dipyridine, and as a consequence of its potential participation in the structure as the neutral dpa, the protonated Hdpa$^+$ or H$_2$dpa^{+2}, or even the deprotonated (NC$_5$H$_4$−N−C$_5$H$_4$N)$^{1-}$ forms.[28−30] As part of these studies, we have isolated the first two members of this family of materials, the two-dimensional [M(Hdpa)$_2$V$_4$O$_{12}$] (M = Co (**1**) and Ni (**2**)).

Experimental Section

Reagents were purchased from Aldrich Chemical Co. and used without further purification. All syntheses were carried out in 23 mL poly(tetrafluoroethylene)-lined stainless steel containers under autogenous pressure. The reactants were stirred briefly before heating. Water was distilled above 3.0 Ω in-house using a Barnstead model 525 Biopure Distilled Water Center.

Preparation of [Co(Hdpa)V$_4$O$_{12}$] (1). A mixture of CoCl$_2$·6H$_2$O (0.088 g, 0.37 mmol), NaVO$_3$ (0.090 g, 0.74 mmol), 4,4′-dipyridylamine (0.127 g, 0.74 mmol), and H$_2$O (10.0 g, 555.6 mmol) in the mole ratio 1:2:2:1500 was heated for 34 h at 120 °C. After the mixture was cooled to room temperature, pink needles of **1** were collected in 60% yield along with unreacted dpa and an amorphous brown powder. Anal. Calcd for C$_{20}$H$_{20}$CoN$_6$O$_{12}$V$_4$: C, 30.0; H, 2.50; N, 10.5. Found: C, 30.2; H, 2.60; N, 10.3.

Preparation of [Ni(Hdpa)V$_4$O$_{12}$] (2). A mixture of NiCl$_2$6H$_2$O (0.088 g, 0.37 mmol), NaVO$_3$ (0.090 g, 0.74 mmol), 4,4′-dipyridylamine (0.127 g, 0.74 mmol), and H$_2$O (10.0 g, 555.6 mmol) in the mole ratio 1:2:2:1500 was heated for 34 h at 120 °C. After the mixture was cooled to room temperature, compound **1** was isolated as green blocks in 70% yield along with small amounts of unreacted dpa and a yellow amorphous solid. Anal. Calcd for C$_{20}$H$_{20}$N$_6$NiO$_{12}$V$_4$: C, 30.0; H, 2.50; N, 10.5. Found: C, 29.8; H, 2.55; N, 10.3.

X-ray Crystallography. Structural measurements of **1** and **2** were performed on a Bruker SMART-CCD diffractometer at a temperature of 150 ± 1 K using graphite monochromated Mo Kα radiation (λ(Mo Kα) = 0.710 73 Å). Crystals of **1** were thin needles (0.08 mm × 0.08 mm × 0.27 mm) with weak diffraction profiles. Consequently, 45 s frame collection times were required in this case. The data were corrected for Lorentz and polarization effects. The structures were solved by direct methods.[31] In all cases, all non-hydrogen atoms were refined anisotropically. Neutral atom scattering factors were those of Cromer and Waber,[32] and anomalous dispersion corrections were taken from Creagh and McAuley.[33] All calculations were performed using the SHELXTL[34] crystallographic software packages.

Table 1. Summary of Crystallographic Data for the Structures of [Co(Hdpa)$_2$V$_4$O$_{12}$] (**1**) and [Ni(Hdpa)$_2$V$_4$O$_{12}$] (**2**)

	1	**2**
chemical formula	C$_{10}$H$_{10}$Co$_{0.5}$N$_3$O$_6$V$_2$	C$_{10}$H$_{10}$N$_3$Ni$_{0.5}$O$_6$V$_2$
fw	399.56	399.45
space group	$P2_1/c$	$P2_1/c$
a, Å	10.388(1)	10.3815(2)
b, Å	7.6749(7)	7.7044(2)
c, Å	16.702(2)	16.6638(4)
β, (deg)	102.516(1)	102.573(1)
V, Å^3	1300.0(2)	1300.86(5)
Z	4	4
D_{calc}, g cm^{-3}	2.042	2.040
temp, K	150(2)	150(2)
λ, Å	0.710 73	0.710 73
μ, cm^{-1}	20.86	21.71
R1[a]	0.0678	0.0471
wR2[b]	0.1184	0.1052

[a] $R = \sum|F_o - F_c|/\sum|F_o|$. [b] $R_w = [\sum w(F_o|^2 - |F_c|^2)^2/\sum w(|F_o|^2)^2]^{1/2}$.

Table 2. Selected Bond Lengths (Å) and Angles (deg) for **1** and **2**

Co−O(1)	2.120(5) × 2	Ni−O(1)	2.133(15) × 2
Co−O(6)	2.046(5) × 2	Ni−O(6)	2.104(3) × 2
Co−N(1)	2.117(5) × 2	Ni−N(1)	2.077(3) × 2
V1−O(1)	1.635(5)	V1−O(1)	1.639(3)
V1−O(2)	1.781(4)	V1−O(2)	1.784(3)
V1−O(3)	1.617(6)	V1−O(3)	1.708(18)
V1−O(4)	1.847(8)	V1−O(4)	1.857(5)
V2−O(2)	1.781(4)	V2−O(2)	1.787(3)
V2−O(4)	1.807(8)	V2−O(4)	1.809(5)
V2−O(5)	1.613(9)	V2−O(5)	1.625(16)
V2−O(6)	1.633(5)	V2−O(6)	1.631(6)
Co−O1−V(1)	159.7(3)	Ni−O1−V1	159.1(2)
V1−O2−V2	172.5(4)	V1−O2−V2	173.7(2)
V1−O4−V2	139.6(5)	V1−O4−V2	140.0(3)
Co−O6−V2	160.9(4)	Ni−O6−V2	148.7(6)
H3N···O4	2.045	H3N···O4	1.922
H2N···O3	2.310	H2N···O3	2.131
		H2N···O5	2.102

Crystallographic details for the structures of **1** and **2** are summarized in Table 1. Atomic positional parameters, full tables of bond lengths and angles, and anisotropic temperature factors are available in the tables in Supporting Information. Selected bond lengths and angles for **1** and **2** are given in Table 2.

Results and Discussion

Although solid-state oxides have conventionally been prepared through high-temperature solid-state reactions, intermediate-temperature synthetic techniques, which include hydrothermal methods,[35−39] have been developed recently and demonstrated to be effective in the isolation of materials such as molybdenum oxides,[17,40] metal halide and pseudohalide phases,[41,42] and metal

(24) Laskoski, M. C.; LaDuca, R. L., Jr.; Rarig, R. S., Jr.; Zubieta, J. *J. Chem. Soc., Dalton Trans.* **1999**, 3467.
(25) Hagrman, D.; Hagrman, P. J.; Zbuieta, J. *Angew. Chem., Int. Ed. Engl.* **1999**, *38*, 3165.
(26) Zapf, P. J.; Hammond, R. P.; Haushalter, R. C.; Zubieta, J. *Chem. Mater.* **1998**, *10*, 1366.
(27) Zapf, P. J.; Warren, C. J.; Haushalter, R. C.; Zubieta, J. *Chem. Commun.* **1997**, 1543.
(28) Zapf, P. J.; LaDuca, R. L., Jr.; Rarig, R. S., Jr.; Johnson, K. M., III; Zubieta, J. *Inorg. Chem.* **1998**, *37*, 3411.
(29) LaDuca, R. L., Jr.; Rarig, R. S., Jr.; Zapf, P. J.; Zubieta, J. *Inorg. Chim. Acta* **1999**, *292*, 131.
(30) Cotton, F. A.; Daniels, L. M.; Jordan, G. T., IV; Murillo, C. A. *Polyhedron* **1998**, *17*, 589.
(31) *SHELXTL PC*; Siemens Analytical X-Ray Instruments: Madison, WI, 1993.
(32) Cromer, D. T.; Waber, J. T. *International Tables for X-ray Crystallography*; Kynoch Press: Birmingham, England, 1974; Vol. IV.
(33) Creagh, D. C.; McAuley, J. W. J. *International Tables for X-ray Crystallography*; Kluwer Academic: Boston, 1992; Vol. C, Table 4.2.6.8.
(34) Sheldrick, G. M. *SHELXTL PC. Structure Determination Programs*, version 5.0; Siemens Analytical Systems: Madison, WI, 1994.
(35) Stein, A.; Keller, S. W.; Mallouk, T. E. *Science* **1993**, *259*, 1558.
(36) Rabenau, A. *Angew. Chem., Int. Ed. Engl.* **1985**, *24*, 1026.
(37) Laudise, R. A. *Chem. Eng. News* **1987**, September 28, 30.
(38) Gopalakrishnan, J. *Chem. Mater.* **1995**, *7*, 1265.
(39) Barrer, R. M. *Hydrothermal Chemistry of Zeolites*; Academic Press: New York, 1982.
(40) Hagrman, D.; Zubieta, J. *Trans. ACA* **1998**, *33*, 109.

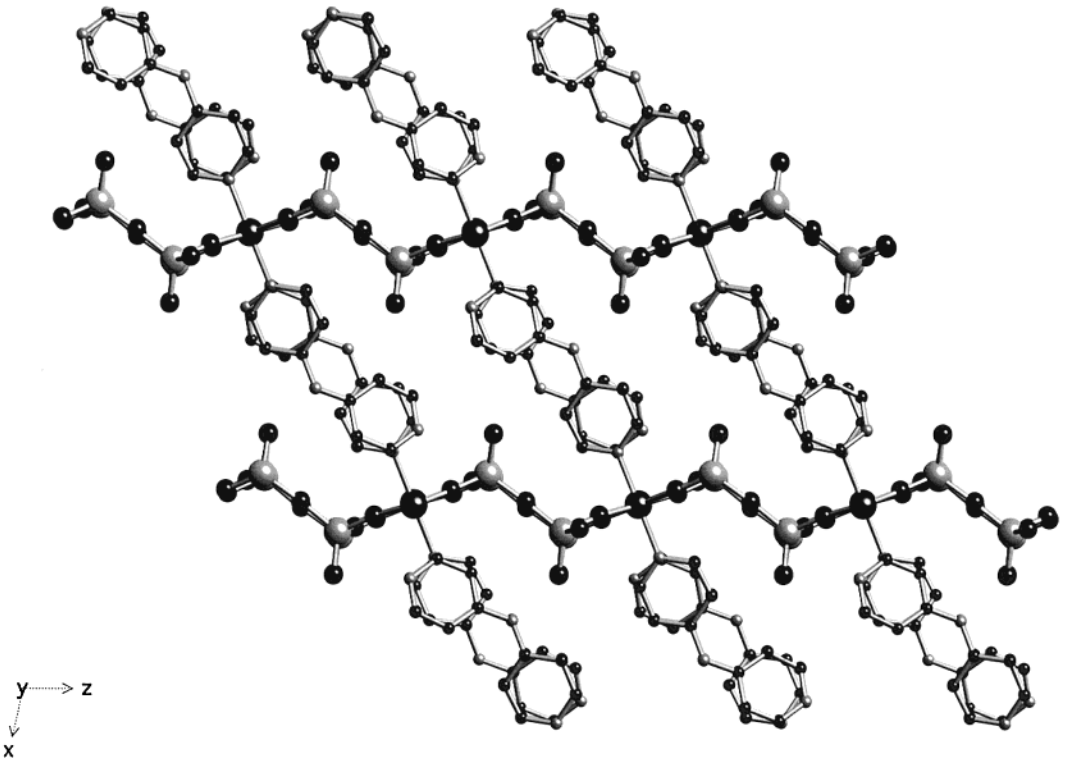

Figure 1. View parallel to the crystallographic *b* axis of the stacking of layers in **1**. Note the interdigitation of the $Hdpa^+$ groups and the alternating organic−inorganic layers.

phosphate and phosphonate materials.[43,44] The exploitation of this "chimie douce" technique offers a number of advantages. The reaction temperatures are sufficiently mild to retain the structural integrity of the starting materials, including organic ligands or templates, thus offering the potential for a modular approach to solid-state synthesis. The reduced viscosity of water under these conditions promotes solvent extraction of solids and crystal growth from solution. Of particular benefit from the viewpoint of organic−inorganic hybrid materials is the ready solubilization of both organic and inorganic starting materials to alleviate differential solubility problems. The hydrothermal parameter space of stoichiometry, temperature, pressure, pH, fill volume, starting materials, templates, and mineralizers affords significant flexibility under conditions for the isolation of both molecular complexes and solid-phase materials for a given compositional system.

We have sought to extend the structure-directing role of organic molecules in inorganic oxide synthesis by exploiting the incorporation of the organic as a ligand to a secondary metal site. The secondary metal−ligand coordination complex cation provides charge compensation for the negatively charged oxide substructure, as well as fulfilling space filling and structure-modifying roles. This secondary metal−ligand subunit exhibits considerable structural versatility depending on the coordination preferences of the metal and the ligand geometry. Consequently, this subunit may be present as isolated coordination cations, one-, two-, or three-dimensional substructures, or integral components of bimetallic oxide phases.

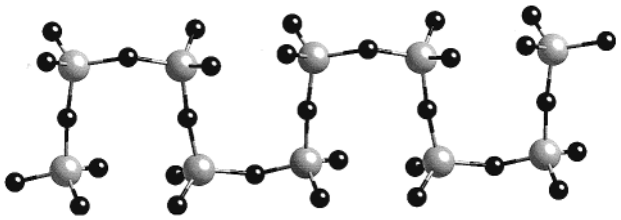

Figure 2. Vanadate chain, which provides one structural subunit of the bimetallic oxide network of **1**.

These general considerations influenced the syntheses of **1** and **2**. The preparations exploited hydrothermal conditions and the affinity of M(II) cations for pyridyl nitrogen donors. The reactions of $MCl_2 \cdot 6H_2O$ (M = Co and Ni), $NaVO_3$, 4,4′-dipyridylamine, and H_2O in the mole ratio 1:2:2:1500 under mildly acidic conditions (pH = 5.5) yielded after 34 h at 120 °C the vanadate phases $[Co(Hdpa)_2V_4O_{12}]$ (**1**) and $[Ni(Hdpa)_2V_4O_{12}]$ (**2**) in good yields. Both compounds exhibited strong IR bands in the range 920−960 cm^{-1} attributed to ν(V═O), and a series of bands in the 1200−1500 cm^{-1} region associated with the ligand.

As shown in Figure 1, the structure of $[Co(Hdpa)_2V_4O_{12}]$ consists of ruffled bimetallic oxide $\{CoV_4O_{12}\}_n^{2n-}$ layers with $Hdpa^+$ groups projecting into the interlamellar region. The $Hdpa^+$ subunits from adjacent layers interdigitate as shown in Figure 1a.

The layers have as their fundamental motif a folded $\{VO_3\}_n^{n-}$ chain of corner-sharing tetrahedra, shown in Figure 2. Each $\{VO_4\}$ tetrahedron thus exhibits two oxo groups that are not utilized in chain linkage. One oxo group from each $\{VO_4\}$ tetrahedron is used to bridge to the octahedral $\{CoO_4N_2\}^{2+}$ sites, while the remaining oxo group is terminal and projects into the interlamellar region. Consequently, the oxide substructure of **1**

(41) (a) Francis, R. J.; Halasyamani, P. S.; O'Hare, D. *Angew Chem., Int. Ed. Engl.* **1998**, *37*, 2214. (b) Mitzi, D. *Chem. Mater.* **1996**, *8*, 791. (c) DeBord, J. R. D.; Lu, Y.-J.; Warren, C. J.; Haushalter, R. C.; Zubieta, J. *Chem. Commun.* **1997**, 1365.
(42) (a) Chesnut, D. J.; Kusnetzow, A.; Zubieta, J. *J. Chem. Soc., Dalton Trans.* **1998**, 4081. (b) Chesnut, D. J.; Zubieta, J. *Chem. Commun.* **1998**, 1707. (c) Chesnut, D. J.; Kuznetzow, A.; Birge, R. R.; Zubieta, J. *Inorg. Chem.* **1999**, *38*, 2663.
(43) Feng, P.; Bu, X.; Stuck, G. D. *Nature* **1997**, *388*, 735.
(44) Khan, I.; Zubieta, J. *Prog. Inorg. Chem.* **1995**, *43*, 1.

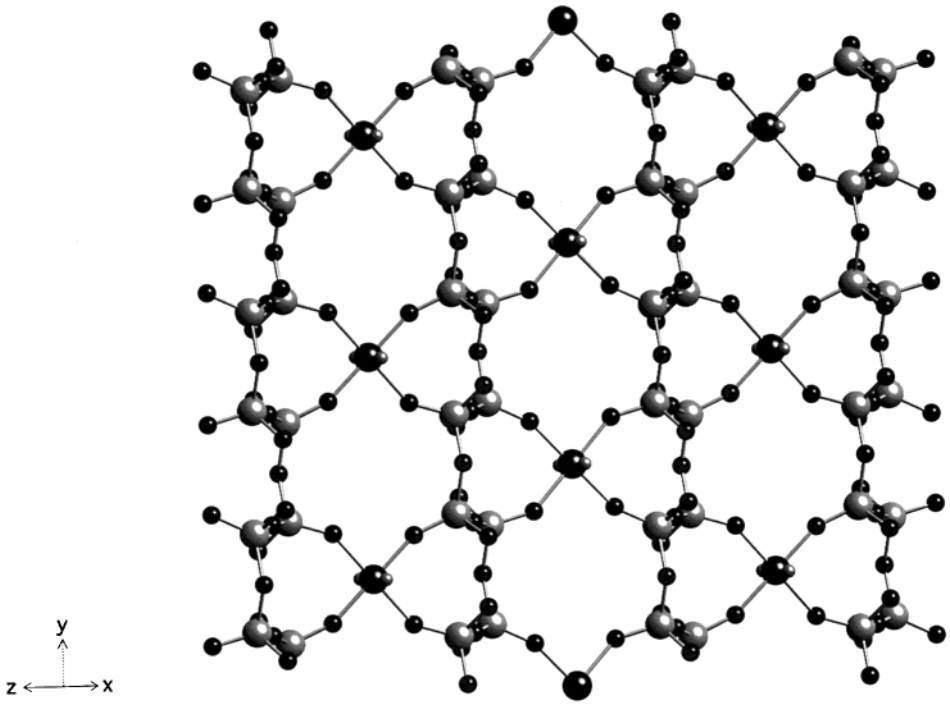

Figure 3. View of the bimetallic oxide network $\{CoV_4O_{12}\}_n^{2n-}$ of **1**.

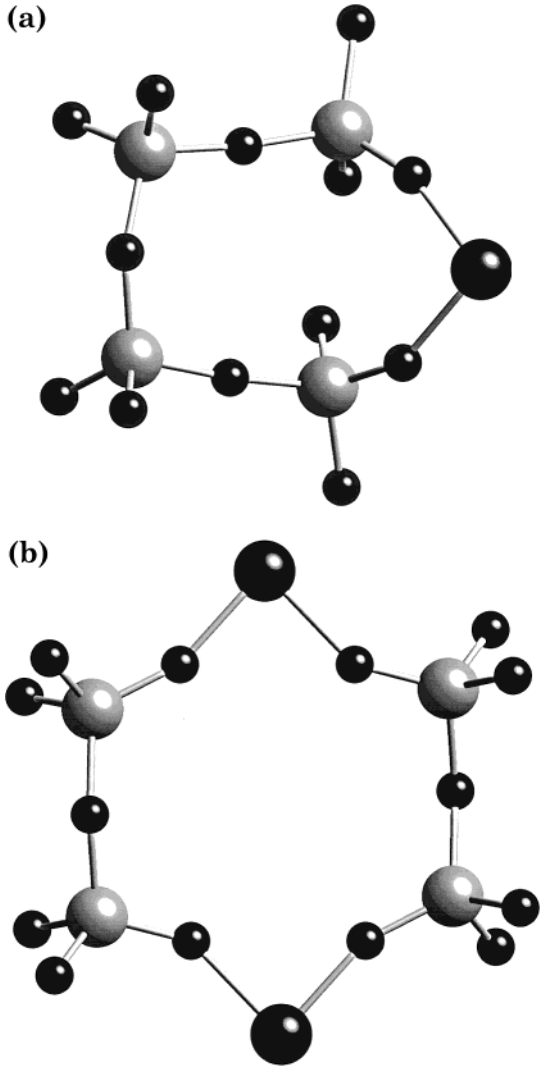

Figure 4. $\{CoV_4O_5\}$ ring (a) and $\{Co_2V_4O_6\}$ ring (b) of the oxide layer of **1**.

is constructed from $\{VO_3\}_n^{n-}$ chains linked through $\{CoO_4N_2\}^{2+}$ octahedra into a bimetallic oxide network, shown in Figure 3.

Each Co(II) center is coordinated to four oxo groups in a planar arrangement, two from each of two adjacent vanadate chains. Each Co(II) site is linked not to adjacent corner-sharing vanadium sites (V−O−V linked) on one chain but to two adjacent vanadium sites on each of two adjacent chains that are not directly linked through polyhedral vertexes but rather brought into proximity by the folding of the vanadate chains. Consequently, the bimetallic oxide network displays two distinct cyclic submotifs, a ten-membered $\{CoV_4O_5\}$ ring and a 12-membered $\{Co_2V_4O_6\}$ ring, shown in Figure 4.

The coordination geometry at each Co(II) site is completed by two axial pyridyl nitrogen donors, one from each of two 4,4′-Hdpa ligands that project outward from both faces of the oxide network. The pendant pyridyl nitrogen is protonated as required by charge-balance consideration. The proton was located on the final difference Fourier maps and refined unexceptionally.

As shown in Figure 5, the interdigitation of the $Hdpa^+$ groups from adjacent layers disposes the ligands above and below the network cavities produced by the $\{Co_2V_4O_6\}$ rings. The $Hdpa^+$ proton is hydrogen-bonded to the O4 oxo group of the adjacent layer.

The structure of the Ni(II) derivative $[Ni(Hdpa)_2V_4O_{12}]$ (**2**) is isomorphous with **1**. As shown in Table 2, the metrical parameters for the structures are unexceptional and the Ni−N distances are shorter than the Co−N counterparts, as anticipated from the trends in covalent radii across the first transition series.

It is instructive to compare the structures of **1** and **2** with that of the previously reported members of the secondary metal−dpa−vanadate family, $[Cu(dpa)VO_3]$.[16] As shown in Figure 6, the structure of $[Cu(dpa)VO_3]$ is also a 2-D bimetallic oxide network. However, the fundamental building block in this case consists of chains of corner-sharing $\{VO_4\}$ tetrahedra linked to $\{Cu(dpa)\}_n^{n+}$ chains, in a parallel double-chain arrangement. Several observations are relevant. The structure of $[Cu(dpa)VO_3]$ reflects in part the coordination preferences of the Cu(I)

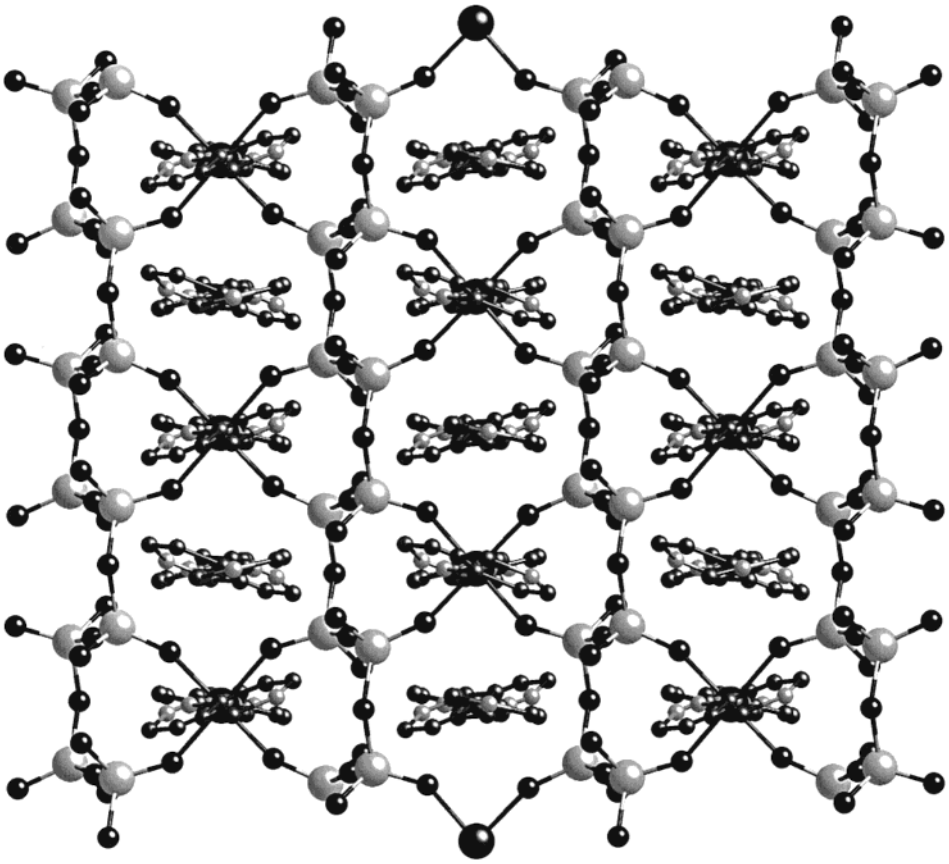

Figure 5. View of the layer structure of **1**, showing the location of $Hdpa^+$ ligands from adjacent layers.

secondary metal site, which in this case adopts $\{CuN_2O\}$ trigonal planar geometry in the motif described above and $\{CuN_2O_2\}$ tetrahedral geometry in the cross-linking chains. It is also noteworthy that the synthesis of $[Cu(dpa)VO_3]$ was carried out under basic conditions (1 equiv of Et_4NOH for 2 equiv of $NaVO_3$) to avoid protonation of the dpa ligand. The dpa is then effective in the common role of a dipodal bridging group in the construction of one-dimensional submotifs with the secondary metal center. Finally, the structural influences of the secondary metal−ligand component on the vanadium oxide substructure are apparent in the contrasting vanadate chain foldings of **1** and $[Cu(dpa)VO_3]$.

The thermal gravimetric analyses of **1** and **2** exhibit a weight loss corresponding to a water molecule between about 300 and 400 °C followed by rapid loss of the ligand in two steps between 400 and 550 °C to give an amorphous gray-blue powder analyzing for NiV_2O_6. The initial weight loss appears to conform to a dehydration, yielding blue-green crystals analyzing for $[M(dpa)_2V_4O_{11}]$. The poor diffraction properties of this material have precluded further analysis. However, a compound of identical composition may be prepared under basic conditions from the hydrothermal reaction of $NiCl_2 \cdot 6H_2O$, $NaVO_3$, and 4,4′-dpa. It is anticipated that appropriate conditions for crystal growth will be established. It is tempting to speculate that $[M(dpa)_2V_4O_{11}]$ may exhibit a $\{M(dpa)_2\}_n^{2n+}$ network and a $\{V_4O_{11}\}^{2-}$ cluster substructure, similar to that recently encountered for the molybdate species $[\{Ni(3,3'\text{-bpy})_2\}_2Mo_4O_{14}]$.[45]

Conclusions

Hydrothermal synthesis offers an effective method for the preparation of organic−inorganic hybrid materials. The modification of the inorganic oxide microstructure by appropriate organic components provides a powerful technique for the design of new materials. However, it is now apparent that the role of the organic subunit of such composite materials is not necessarily limited to that of leaving a molecular-sized void in the inorganic oxide backbone upon postsynthesis removal, as in the zeolites, but rather extends to an essential synthetic function. When an appropriate structural motif possessing a suitable shape and charge-to-volume ratio is provided, the organic component can influence crystal growth via charge neutralization at the crystal−solution interface. The incorporation of a structurally tailored organic molecule will introduce a significant degree of structural complexity into the system as a result of the relatively large number of oxide skeletal atoms required to accommodate the organic component. This general strategy has now been elaborated by the introduction of structural subunits consisting of coordination complex cations, which are incorporated into the anionic metal oxide microstructure and which serve to direct the structural characteristics of the oxide.

Structures such as **1** and **2** exhibit a hierarchical order and complexity. Such structures are kinetically, rather than thermodynamically, stable, providing an intrinsic dynamic nature that enhances the fundamental complexity of such hybrid materials.[46] Since functionality of materials is related to their structural complexity,[47] one approach to the design of new materials with useful physical properties exploits the organic−inorganic interface to modify the microstructure of the phase.

On the other hand, such complexity limits the degree of predictability of the product structure and composition. While

(45) LaDuca, R. L., Jr.; Desciak, M.; Laskoski, M.; Rarig, R. R., Jr.; Zubieta, J. Unpublished results.

(46) Olson, G. B. *Science* **1997**, *277*, 1237.

(47) Whitesides, G. M.; Ismagilov, R. F. *Science* **1999**, *284*, 89.

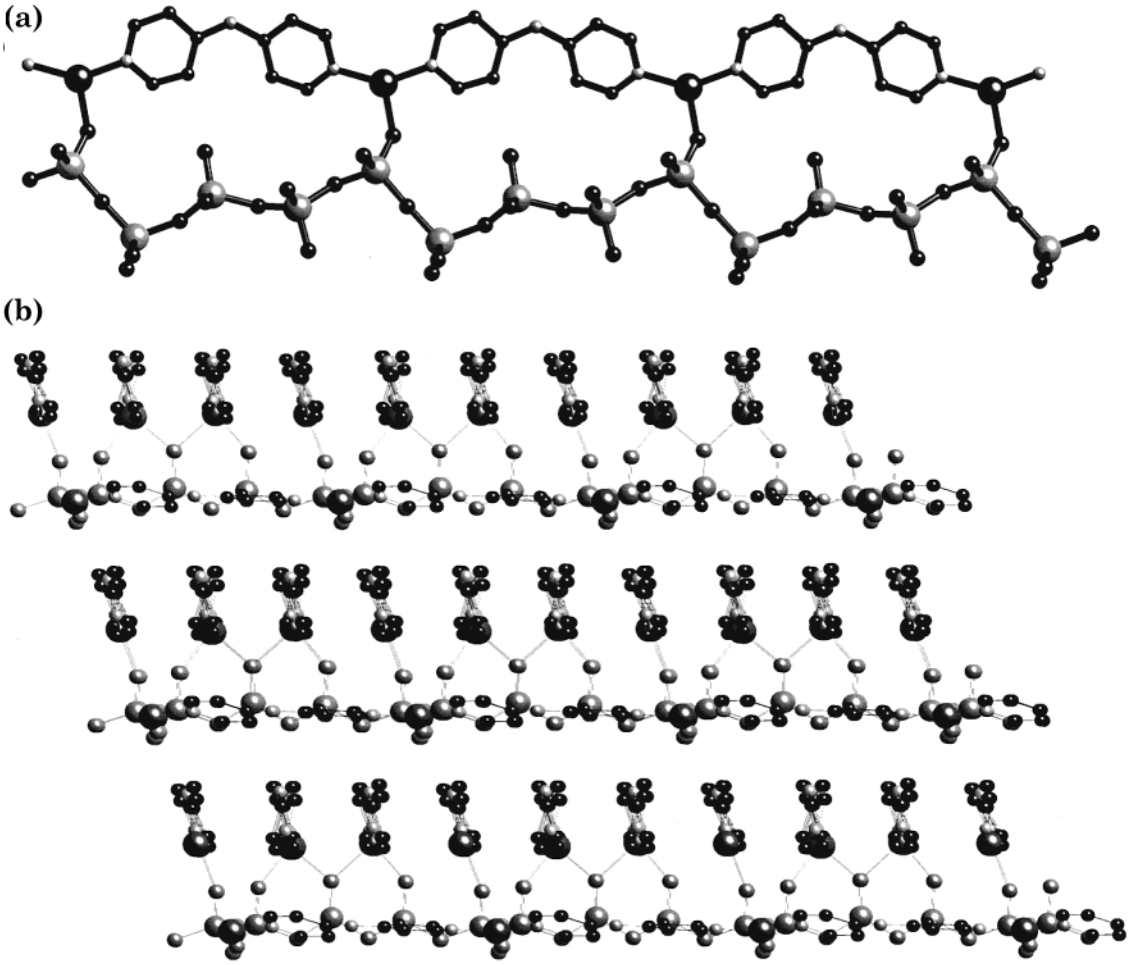

Figure 6. (a) View of the $\{Cu(dpa)V_4O_{12}\}_n^{3n-}$ double chain of $[Cu(dpa)VO_3]$. (b) View of the overall structure of $[Cu(dpa)VO_3]$.

such complexity hinders the rational design of materials, it does not necessarily render solid-state inorganic materials undesignable. As the products of empirical development are characterized, structure−function relationships are manifested, providing a reciprocity for further design.

Acknowledgment. This work was supported by NSF Grant CHE9987471. The work at King's College was supported by a grant from the Research Corporation.

Supporting Information Available: X-ray crystallographic files in CIF format for structures **1** and **2**; XRD patterns of $[Ni(Hdpa)_2V_4O_{12}]$ (**2**), of **2** dehydrated at 380 °C, and of **2** after being heated to 720 °C); TGA plots for $[Ni(Hdpa)_2V_4O_{12}]$ from room temperature to 550 °C and from room temperature to 700 °C. This material is available free of charge via the Internet at http://pubs.acs.org.

IC000224I